Zurich University
of Applied Sciences

School of
Engineering

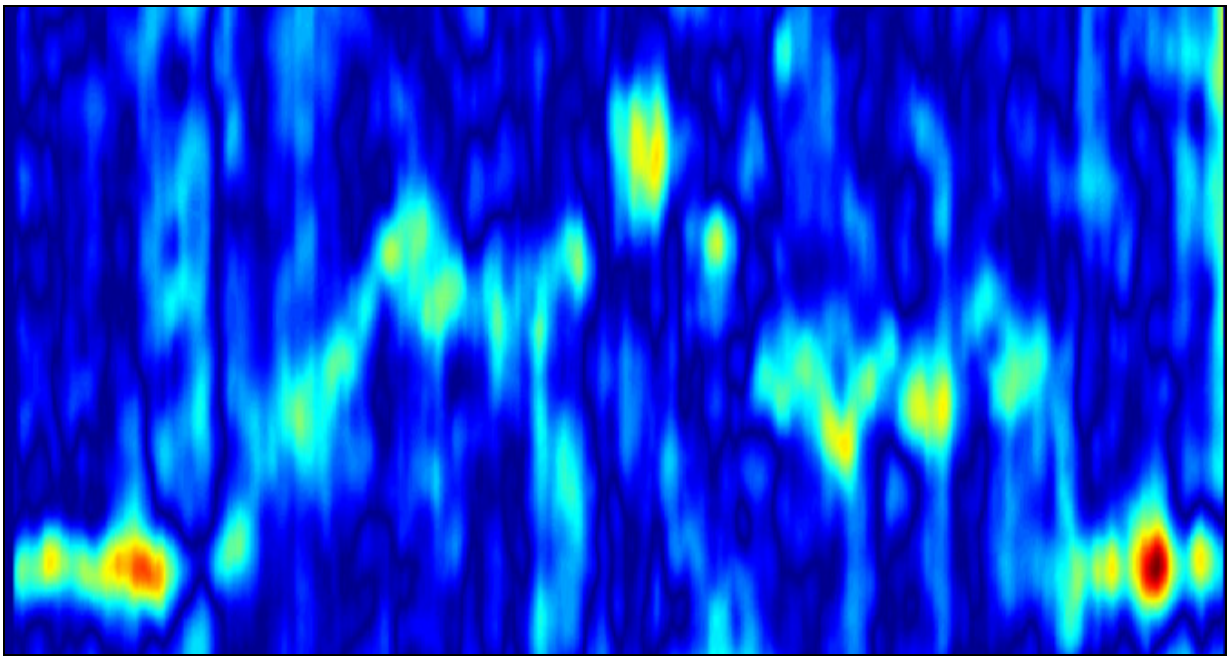

New Methods for Travel Time Estimation on Freeway Sections

Albert Steiner
Beate Sick

MOTION
Working Papers Transportation Systems

School of Engineering
ZHAW Zurich University of Applied Sciences

New Methods for Travel Time Estimation on Freeway Sections

Albert Steiner, Beate Sick

Zurich University of Applied Sciences

School of Engineering, MOTION No. 1, June 2008

Abstract:

In this paper we present two novel approaches to estimate the travel times between subsequent detector stations in a freeway network, with long distances between detector stations and several unobserved on- and off-ramps.
The network under investigation is a two-lane freeway. The maximum distance between detector stations, for which travel times were estimated is about 20 km with four unobserved on- and off-ramps in between.
The algorithms were applied on real data sets, which has led to reasonable estimates. However, due to unknown actual ('true') travel times, a performance assessment was not possible. The algorithms were also applied on simulated data with known travel times. This allowed the verification of the estimated travel times. The simulated data were generated by the microscopic traffic simulation tool AIMSUN NG®. The detector stations were assumed to be equipped with widespread double loop detectors, i.e., for each vehicle, the only information used was its length (with a superimposed measurement noise) and the arrival time at the detector stations.
The estimated travel times show that with both methods all relevant travel time characteristics were correctly identified for the investigated scenarios. Moreover, a comparison of the estimates with the actual travel times has shown very good accuracy.
Besides the fact that the methods work well even under hindered conditions (long distance, unobserved ramps), some additional practical benefits are: provided that single car data are available with sufficient accuracy, no additional investments are required; both methods work fully anonymous; extensions to more sophisticated detection technologies that provide additional vehicle features are straightforward; the travel time estimates form a good basis for any travel time prediction method.

Keywords:

travel time estimation – freeway traffic – pattern recognition – image processing – global sequence alignment

Quotation:
Steiner, A. and B. Sick (2008) New Methods for Travel Time Estimation on Freeway Sections, *MOTION – Working Papers Transportation Systems*, 1, School of Engineering, ZHAW, Winterthur.

1. Introduction

The knowledge of travel times on road networks is of vital importance, both for network operators and drivers. *Operators* can use travel time information (current and/or predicted) to improve the control of their networks. *Drivers* can select their optimal route, either pre-trip or en-route, based on the travel time information available and the drivers' individual preferences. For *transport companies* the knowledge of travel time helps to increase their delivery service quality. Moreover, they can choose their routes dynamically according to the current and predicted traffic state and thus increase their efficiency.

The distribution of the information can be done either by collective information channels (e.g., variable message signs (VMS), radio (incl. Traffic Message Channel TMC)), or by individual information services (e.g., mobile service applications).

In the last decades, various methods were developed for travel time estimation and prediction. The focus of the presented paper is on travel time estimation, i.e. the online estimation of travel times for vehicles from data provided by local detector stations with double inductance loops.

Based on the vehicle length provided by double inductance loops, Coifman and co-workers (Coifman (1998a, 1998b, 2002), Coifman and Cassidy (2002), Coifman and Ergueta (2003), Coifman and Krishnamurthy (2007)) as well as Abdulhai and Tabib (2003) and others have made important contributions during the last decade. Other approaches use raw vehicle signatures from inductance loops (e.g., Pfannerstill (1984), Kwon (2006)). However, signature data are in general not available, or only with additional infrastructure investments.

It is important to note here, that by using loop detectors, no distinct vehicle reidentification is possible.

One of the selling points of the methods presented here is, that they can applied on many freeway sections, since loop detectors are widely used. Thus, provided that single car data are available online and in sufficient quality (i.e. small length measurement error, no bias), no additional infrastructure investments are required. Furthermore, both methods work fully anonymous and therefore no violations of privacy arise. Finally, extensions to more sophisticated detection technologies that provide additional vehicle features are straightforward, but will not be investigated in this work.

2. Methods

In this section we present two new methods for travel time estimation on freeway sections. Both methods use only vehicle length and the time stamp per detector station as input data.

2.1 Method 1: Travel time estimation with pattern recognition and image processing

In this section we briefly outline the first approach, which combines pattern recognition and image processing techniques.

2.1.1 Overall procedure

The method presented here aims to estimate the travel time between subsequent detector stations, where only noisy length measurements of individual vehicles are available. We further assume, that the error of the length measurements (i.e., its standard deviation) is known and that it is constant over time. Furthermore, time stamps are captured as the vehicles pass the detector stations.

Figure 1 Overall procedure of the first approach.

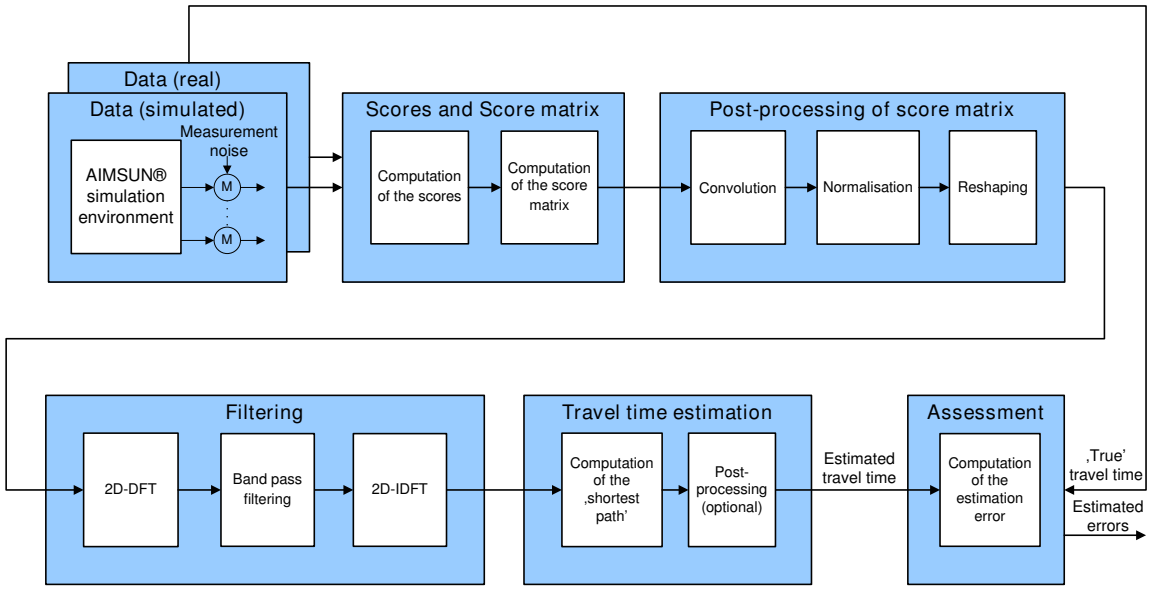

2.1.2 The individual steps

Computation of the scores

A score is calculated for each combination of vehicles i and j observed at the up- and downstream station, respectively:

$$s_{ij} = \underbrace{\alpha_1 \exp\left[-\left(L_i - L_j\right)^2 \Big/ \left(\Delta L_{\text{estim}}\right)^2\right]}_{\substack{\text{Contribution by length comparison} \\ \text{of vehicles } i \text{ and } j}} + \underbrace{\alpha_2 \exp\left[-\left(t_j - t_i - \hat{\tau}_{ij}\right)^2 \Big/ \left(\Delta\tau\right)^2\right]}_{\substack{\text{Contribution by travel time comparison} \\ \text{with 'a priori' information (optional)}}} \quad , \qquad (1)$$

where s_{ij} is the score resulting from the feature comparison of vehicles i (upstream station) and j (downstream station), L_i and L_j denote the measured vehicles lengths at upstream and downstream detector stations, respectively, ΔL_{estim} represents the assumed estimation error of these measurements, with $\Delta L_{\text{estim}} = 2\left|\Delta L_{\text{noise}}\right|$, t_i and t_j denote the time stamps as the vehicles pass the detector stations, $\Delta\tau$ represents the assumed error of 'a priori' travel time estimates, and finally α_1 and α_2 are two weighting factors. Currently we set $\alpha_1 = 1$ and $\alpha_2 = 0$, i.e., only the vehicle length is used to determine the score.

The score matrix: superposition of the scores

Once we have the scores available for each combination of vehicles i and j, we use them to build a score matrix S. This is explained in the following.

The score matrix is of dimension $\left[Y \times X\right]$. The number of rows (X) is equal to the considered arrival time range (7 hours in our case, see Figure 2) divided by time interval (resolution) $\Delta t = 5\,\text{sec}$. Each column x, with $x \in \{1,...,X\}$, represents a time interval $\left[t_x - \Delta t, t_x\right)$ with $t_x = x\Delta t$ and thus $X\Delta t$ is equal to the arrival time range. The number of rows (Y) is equal to the travel time range (depends on OD combination, see Figures 2a to 2d), again divided by Δt. Each row y, with $y \in \{1,...,Y\}$, represents a time interval $\left[t_y - \Delta t, t_y\right)$ with $t_y = y\Delta t$, and thus $Y\Delta t$ is equal to the whole travel time range.

For each ij-combination we know the arrival time of vehicle j at the destination (t_j) and the travel time from $\tau_{ij} = t_j - t_i$. With this, we are now able to determine the cell (given by row y and column x) within score matrix S to which score s_{ij} needs to be added. The column number x results from determining t_x such that $t_x - \Delta t \le t_j < t_x$, i.e., $x = \left\lfloor t_x / \Delta t \right\rfloor$. The row number ($y$) results from determining t_y such that $t_y - \Delta t \le t_j - t_i < t_y$, i.e., $y = \left\lfloor t_y / \Delta t \right\rfloor$. If

more than one score needs to be placed to same cell, the value is simply added to the existing entry. The procedure described above can formally be written as

$$S(x,y) = \sum_{\substack{t_x - \Delta t \le t_j < t_x \\ t_y - \Delta t \le t_j - t_i < t_y}} s_{ij} \qquad \forall\, i \in \mathcal{I}_o,\ j \in \mathcal{J}_d,\ x \in \{1,...,X\},\ y \in \{1,...,Y\}, \tag{2}$$

where $\mathcal{I}_o$ and $\mathcal{J}_d$ denote the number of vehicles that have passed the upstream and downstream detector station, respectively, during the considered arrival time range. All other variables and relations were introduced before.

A visualisation of a score matrix S can be found in Figure 2a. What we see is, that most areas are dark blue, while some are light-blue. The light-blue cells hold higher scores than the dark blue cells and indicate that they include more information. However, with only this information, we cannot estimate any travel time. Therefore some post-processing steps are required, which we briefly explain now.

Post-processing: convolution, normalisation and reshaping

The basic idea of the *convolution* used in this context is to "link" cells with high scores in matrix S. The matrix after the convolution step is shown in Figure 2b. It is obvious that some structures become visible, but it is still no possible, to draw conclusions about the travel time.

In a next step, we perform a *normalisation* of the diagonal elements of the matrix as provided after the convolution step, such that the diagonal cells sum up to one. The result after this procedure is shown in Figure 2c. Again, the information contents increased, which can be see by the revealing "structures". Nonetheless, some further processing is required.

We *reshape* the matrix (image) with dimension $Y \times X$ to an image with dimension $M \times N$. This step was motivated by the fact that, given a certain relation between height and width, the human eye is able to see structures more easily. The assumption was, that we can reveal the same information by using image filters.

Filtering

The filtering step applies a 2nd order 2D-Butterworth band pass on the reshaped image. As we can see in Figure 2d, the resulting image reveals clearly some interesting structures. Areas with light-blue to red indicate that the travel time graph might cross these areas.

Computation of the shortest path

To connect the light-blue to red areas of Figure 2d and thus compute meaningful travel times, we use a shortest path method as follows: For each cell c, processed from left to right (columns) and top to bottom (rows), we search a cell d (left of cell c and within a allowed

vertical range) from which the costs for moving from d to c become minimal. The minimal costs to get to c are stored in a matrix. Once the matrix is computed, we compute the path with the minimal costs by starting at an appropriate cell at the right boundary of the matrix and thus derive the estimated travel time. Examples can be found in Figures 9 b, d, f, and h.

2.1.3 A graphical representation at the different steps

Figure 2 Representation of information at the various steps (a) score matrix, (b) after convolution, (c) after normalisation, (d) after filtering.

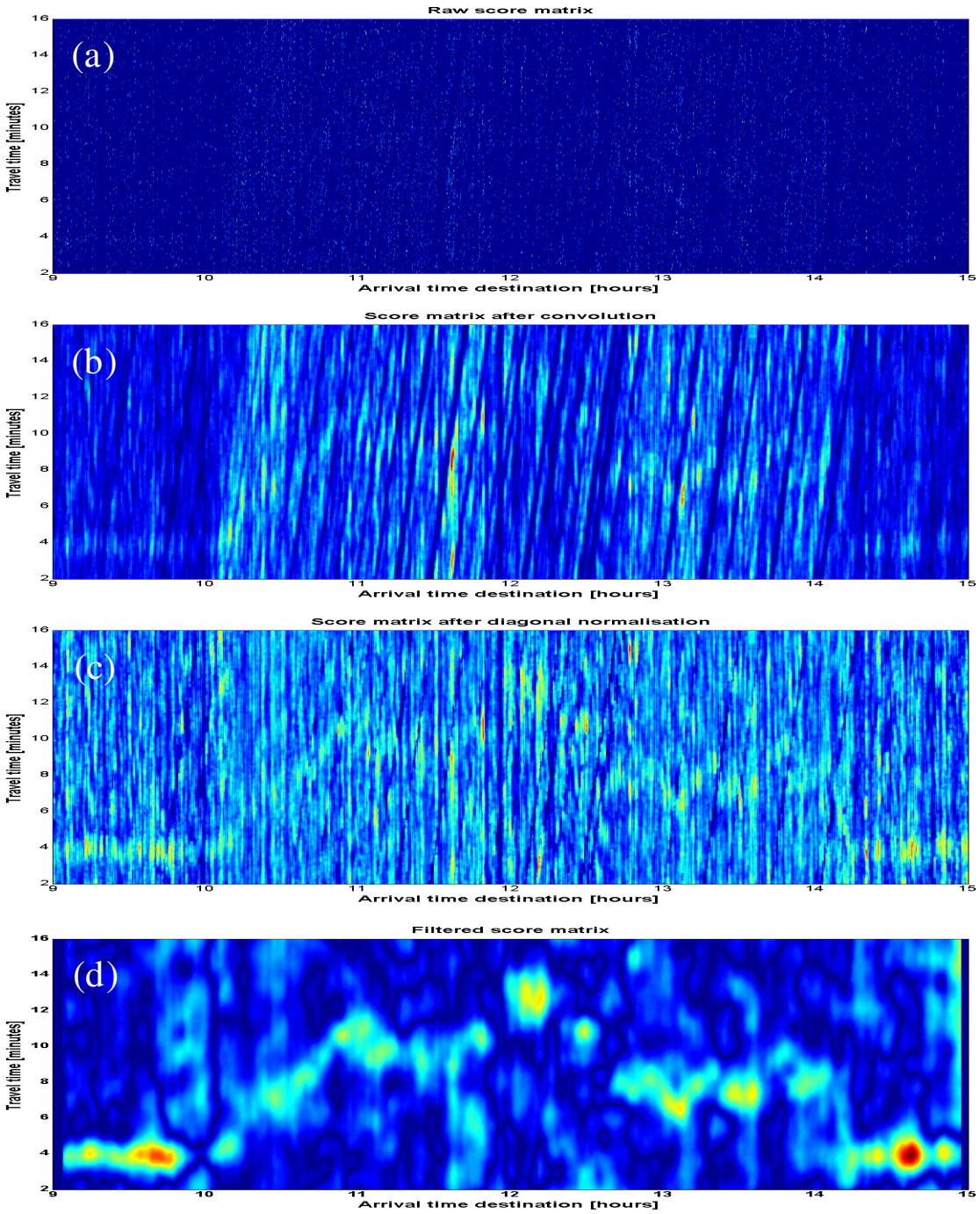

2.2 Method 2: Travel time estimation with global sequence alignment

This part of the paper presents the application of a global alignment algorithm on vehicle data measured at freeway dual-loop detectors to determine the travel. Most existing methods for extracting travel time information from loop detector data rely on matching individual vehicles between detector stations at rather short distances. We will show that a global alignment algorithm which aligns entire vehicle lengths sequences from two subsequent detectors allows us to determine a time resolved travel time estimation. We will demonstrate that this algorithm does even work under difficult conditions like unobserved ramps between the detectors, long detector distances and dense traffic. The utilized method is based on the Needleman-Wunsch algorithm (Needleman-Wunsch], which is well known and frequently used in the field of biological sequence alignment (e.g. DNA sequences, protein sequences). We have adapted the algorithm to align sequence of noisy vehicle length sequences, implemented it in the statistical programming language R, and successfully applied it to real life data and reference data from a microscopic traffic simulation tool.

2.2.1 Overall procedure

Vehicle data from freeway dual-loop detectors provide for each detected vehicle the passing time and the vehicle length. The presented method uses a global alignment algorithm to align the vehicle length sequences, which were recorded at two subsequent detectors (at origin and destination) over several hours. Details of the alignment algorithms are described in the following sections. From the global alignment the time stamps from each matching vehicle pair are extracted, which give directly the arrival time at destination t^D and the travel time between origin and destination as difference of the two time stamps $t^D - t^O$ (see Figure 3).

Figure 3 Overall procedure to determine the travel time from global sequence alignment of lengths sequences measured at an origin and destination detector station. In the global alignment a match is indicated by *M*, a mismatch or substitution by *MM*, a deletion by *Del.*, and an insertion by *Ins.*. The established matches are numerated and the destination passing time t^D and the travel time $t^D - t^O$ is extracted from each match.

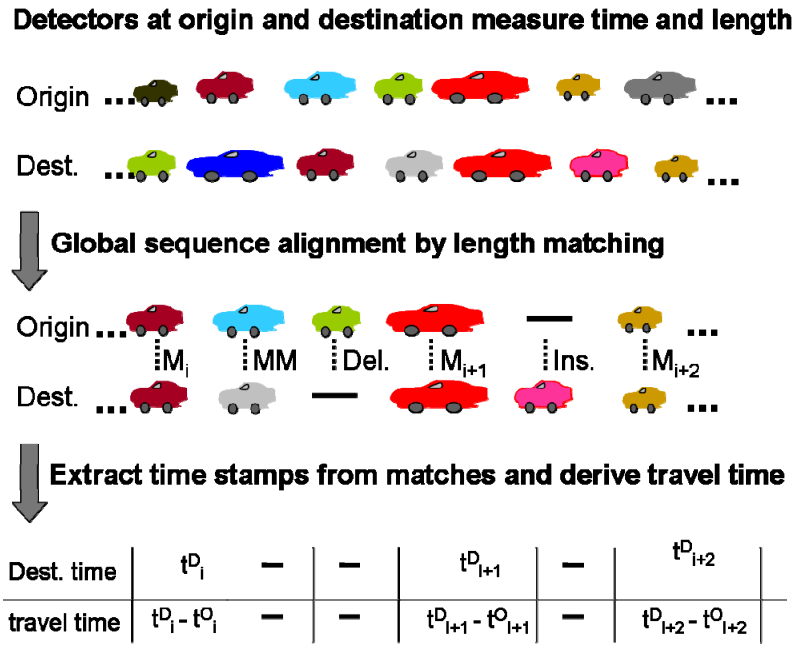

2.2.2 Introduction

Sequence alignment aims on revealing which mutations did lead from an original sequence to a subsequent sequence which has evolved from the origin. It also is pinpointing regions of high similarity in two compared sequences. Most sequence alignment algorithms were developed in the field of bioinformatics for comparing DNA, RNA or Protein sequences. In these cases the sequences consist of a very limited number of different units – in the case of DNA and RNA molecules we have only 4 different bases {A, G, C, T}. Figure 4 shows two different alignments of two DNA sequences.

The general assumption in sequence alignment is that one sequence evolves from the other sequence by the application of a number of simple transformations:

a) Deletion (gap in the second sequence): deletion of an unit in the origin sequence

b) Insertion (gap in the origin sequence): insertion of an unit in the origin sequence

c) Replacement/substitution/mismatch: one unit is replaces another unit

An alignment can be assessed quantitatively when a scoring system is defined. A scoring system defines rewards for matching units and penalties for mismatches or gaps (see Figure 4).

Figure 4 Here two possible alignments of two DNA sequences I and II are visualized. As common in many applications each position in the alignment is scored independently and summed up to determine the score of the entire alignment, e.g. a match may contributes with a score ore reward of +1, a mismatch with a negative score or penalty of -1 and a gap with a penalty of -2.

```
Example:
Sequence I:  GCGCATGGATTGAGCGA
Sequence II: TGCGCCATTGATGACCA
A possible Alignment of sequences I and II:
             - G C G C - A T G G A T T G A G C G A
             T G C G C C A T T G A T - G A C C - A
scoring:   -2+1+1+1+1-1+1+1-1+1+1+1-2+1+1-1+1-2+1   =  4
Resulting score: (+1x13) + (-1x3) + (-2x3) = 4

Another possible Alignment of sequences I and II:
             - - - - - - G C G C A T G G A T T G A G C G A
             T G C G C C - - - - A T T G A T G A C C A - -
Scoring:   -2-2-2-2-2-2-2-2-2-2+1+1-1+1+1+1-1-1-1-1-1-2-2=  -25
Resulting score: (+1x5) + (-1x6) + (-2x12) = -25
```

The goal of alignment is usually to determine that alignment with an optimal overall score.

If two sequences are aligned along their entire lengths the result is called global alignment. Performing a global alignment is reasonable, when we expect that the two sequences are related over their entire lengths. When dealing with partly overlapping sequences, a global alignment that down weights gap penalties at the extremities of the sequences is indicated.

2.2.3 Special considerations for aligning vehicle length sequences

In the case of vehicle sequences we observe a deletion or an insertion if a vehicle has left or entered the observed lane. A replacement implies that one vehicle has left the lane and another car has joined the lane and has taken its place in the sequence.

To decide if two vehicle lengths observed at two subsequent detector stations could stem from the same car, we need to consider the measurement error. The manufacturer of the dual-loop detectors, from which our data are derived, specifies an accuracy of ± 20 cm on lengths measurements. Accordingly, two measured lengths are considered as match if they are equal within the accuracy range.

The length sequence from the first detector station can be given as vector $X_n = (x_1, x_1, ..., x_n)$, where n is the number of detected vehicles, analogously from the second detector we get the length sequence $Y_m = (y_1, y_1, ..., y_m)$ with m detected vehicles. We observe these length sequences at both detector stations during the same time range. This means that the last couple of vehicles which have been observed at the upstream station are not observed at the downstream station, and analogously the first sequence part from the downstream station has no counterpart at the upstream sequence. Therefore an alignment algorithm should be used which is adapted to overlapping sequences and penalizes gaps at the overlapping ends much less than gaps (deletions/insertions) in the sequence interior.

2.2.4 Global alignment based on the Needleman-Wunsch algorithm

Given a scoring scheme, we need to have an algorithm that computes the highest-scoring alignment of two sequences. The Needleman-Wunsch algorithm is a dynamic program that solves the problem to determine the best global alignment of two sequences $X_n = (x_1, x_1, ..., x_n)$ and $Y_m = (y_1, y_1, ..., y_m)$. The basic idea of the algorithm is to build up an optimal alignment using previous solutions for optimal alignments of smaller substrings. The Needleman-Wunsch algorithm mainly defines how to compute an $n \times m$-matrix F in which $F(i, j)$ equals the best score of the alignment of the two substrings $X_i = (x_1, x_1, ..., x_i)$ and $Y_j = (y_1, y_1, ..., y_j)$ (see Figure 5). The lower right diagonal element $F(n, m)$ of this matrix gives then the score of the optimal global alignment of the sequences $X_n = (x_1, x_1, ..., x_n)$ and $Y_m = (y_1, y_1, ..., y_m)$.

Figure 5 Scoring matrix F. a) All other elements $F(i, j)$ are recursively computed from one of their diagonal, above, and left neighbouring elements $F(i-1, j-1)$, $F(i, j-1)$ or $F(i-1, j)$, respectively. The starting point is $F(0,0) = 0$, b) Extension procedure: Each element (i, j) can be reached from three possible prefixes. We choose that way which yields the highest score $F(i, j)$.

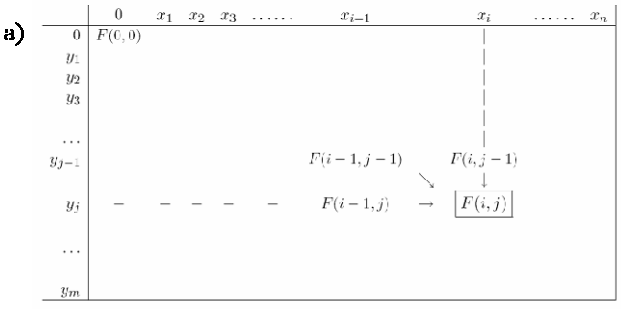

b) Three possible ways to reach the element (i, j):

1) Diagonal way coming from: (i–1, j–1) to (i, j) means that we start from the prefixes X_{i-1} and Y_{j-1} and align x_i against y_j to get an alignment for X_i and Y_i:
$x_1 \ldots x_{i-2}\ x_{i-1}\ x_i$
$y_1 \ldots y_{j-2}\ y_{j-1}\ y_j$
The score of this alignment is: $F(i, j) = F(i-1, j-1) + s(x_i, y_j)$,
where s gives an positive reward, in case of x_i matches y_j or a negative penalty in case of a substitution (mismatch) between x_j and y_j

2) Left way coming from: (i–1, j) to (i, j) means that we start from the prefixes X_{i-1} and Y_j and since y_j is already aligned in Y_j we have to align x_i against a gap:
$x_1 \ldots x_{i-2}\ x_{i-1}\ x_i$
$y_1 \ldots y_{j-1}\ y_j\ -$
The score of this alignment is: $F(i, j) = F(i-1, j) - d$
where d is the penalty for a deletion (gap in the subsequent sequence)

3) Upper way coming from: (i, j–1) to (i, j) means that we start from the prefixes X_i and Y_{j-1} and since x_i is already aligned in X_i we have to align y_j against a gap:
$x_1 \ldots x_{i-1}\ x_i\ -$
$y_1 \ldots y_{j-2}\ y_{j-1}\ y_j$
The score of this alignment: $F(i, j) = F(i, j-1) - d$
where d is the penalty for a insertion (gap in the origin sequence)

Knowing the optimal alignment score, we now turn to the question of how to obtain an actual alignment which has this optimal score. While computing the scores $F(i, j)$ one should also memorize from which of the three possible prefixes the element was reached. Most easily this information is stored in an independent matrix. With this knowledge we can trace back the alignment path which leads to an optimal global alignment (see Figure 6).

Figure 6 Alignment example: Sequence I: A G C , Sequence II: A A A C used scoring system: score (match) = + 1, score (mismatch) = –1, score (gap) = – 2.

Matrix F:

		A	G	C
	0	**1**	**2**	**3**
0	0	-2	-4	-6
A 1	-2	1	-1	-3
A 2	-4	-1	0	-2
A 3	-6	-3	-2	-1
C 4	-8	-5	-4	-1

Element $F(4,3)$ holds the optimal score of -1 of the global alignment of the two sequences. To determine the actual alignment the memorized trace information is used (see red arrows) and we can read of the following optimal alignment:

A G – C
A A A C

2.2.5 From the alignment to a travel time estimation

To determine the travel time between two subsequent detectors stations an optimal global alignment of the length sequences are determined as described above. Then we use the time stamps from each matching vehicle pair, to determine the arrival time at destination t^D and the travel time between origin and destination as difference of the two time stamps $t^D - t^O$ (see Figure 3).

3. Application

3.1 Simulation network

The simulation network under investigation is a section about 20 km long and on the Swiss national freeway A1 (from Bern to Zurich). Figure 7 shows a map with the network and highlighted detector stations. Figure 8 shows the simplified network model.

Figure 7 Real network with detector stations as used for the simulation.

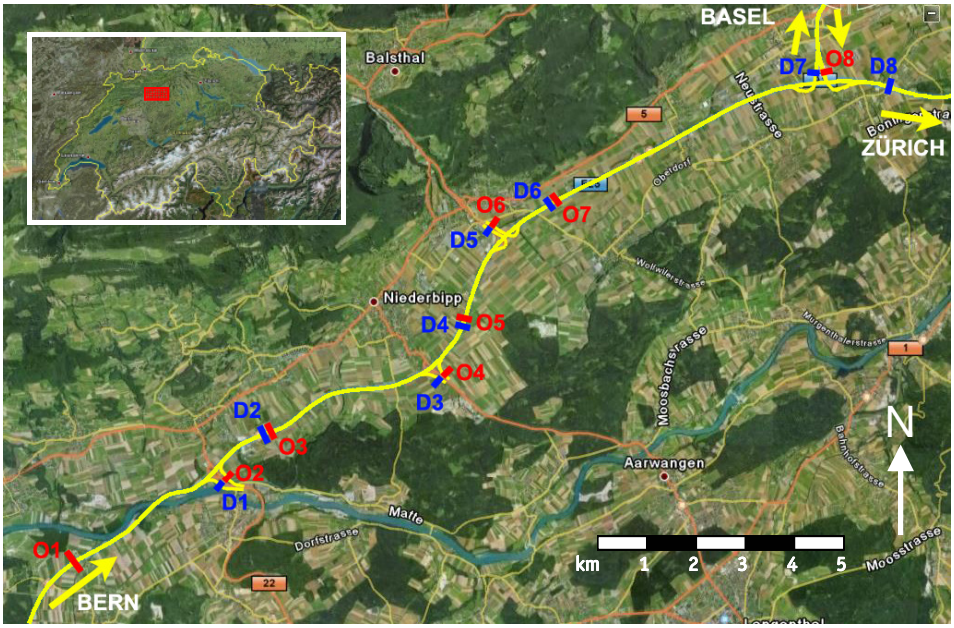

Source: Background by GoogleEarth®, with network data etc. added by the authors

Figure 8 Simplified representation of the network shown in Figure 7.

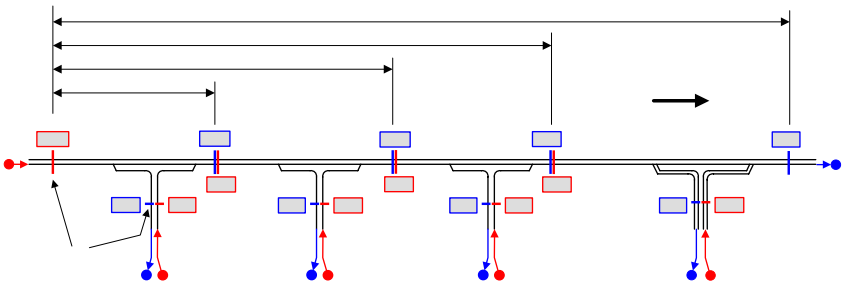

3.2 Detector types

The detectors used on the Swiss freeway network are mainly 'Marksman M660' by Golden River Ltd. According to a distributor (Taxomex (1999)) and Rubin (2007), the accuracy of the length measurements is $\Delta L_{\text{noise}} < \pm 20\,\text{cm}$. Accordingly we conducted simulations with assumed accuracies of $\Delta L_{\text{noise}} = \pm 20\,\text{cm}$.

3.3 Vehicle mix (length distribution)

To feed the simulation with a vehicle mixture that is close to reality, distributions of the lengths at the real detector stations were analysed. From this, we defined vehicle classes together with appropriate properties (e.g., length, driving characteristics (driver, vehicle)) in AIMSUN as part of the simulation input.

3.4 Length measurement error

To simulate the length measurement errors that are experienced in practice, for each vehicle that is generated by the AIMSUN simulation environment, an error will be added to its original length. Based on the assumptions regarding accuracy made in section 3.2, the errors ΔL_{noise} are simulated i.i.d. uniformly distributed between ± 20 cm.

4. Results

4.1 Method 1: Travel time estimation based on pattern recognition and image processing techniques

With an assumed measurement error of $\Delta L_{\text{noise}} = \pm 20\,\text{cm}$, for four origin-destination combinations we show in Figure 9 (i) the filter output together with the estimated travel times (plots on the left side), and (ii) a comparison of the estimated and the actual travel times (plots on the right side).

Figure 9 Estimation results for $\Delta L_{\text{noise}} = \pm 20\,\text{cm}$ and four OD-combinations: O1→D2 (a) Filter output and estimated travel times, (b) Actual and estimated travel times; O1→D4 (c) Filter output and estimated travel times, (d) Actual and estimated travel times; O1→D6 (e) Filter output and estimated travel times, (f) Actual and estimated travel times; O1→D8 (g) Filter output and estimated travel times, (h) Actual and estimated travel times.

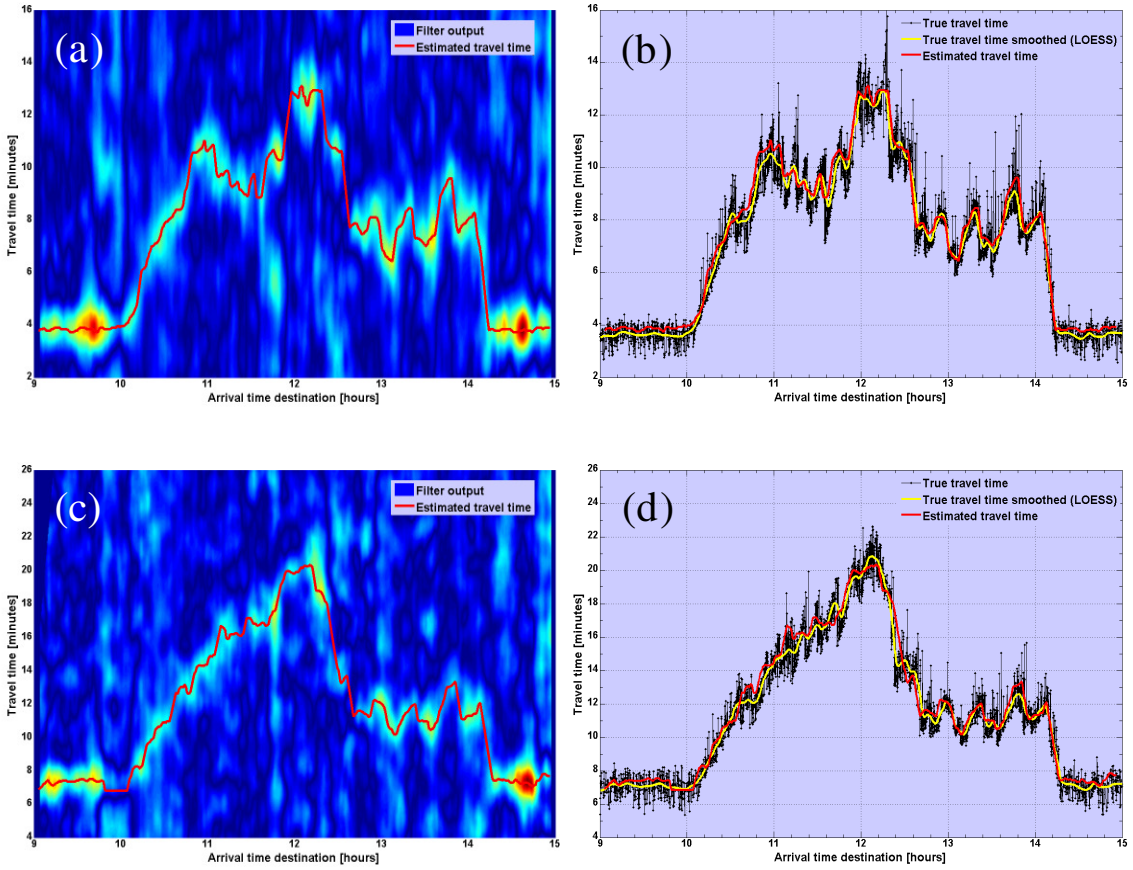

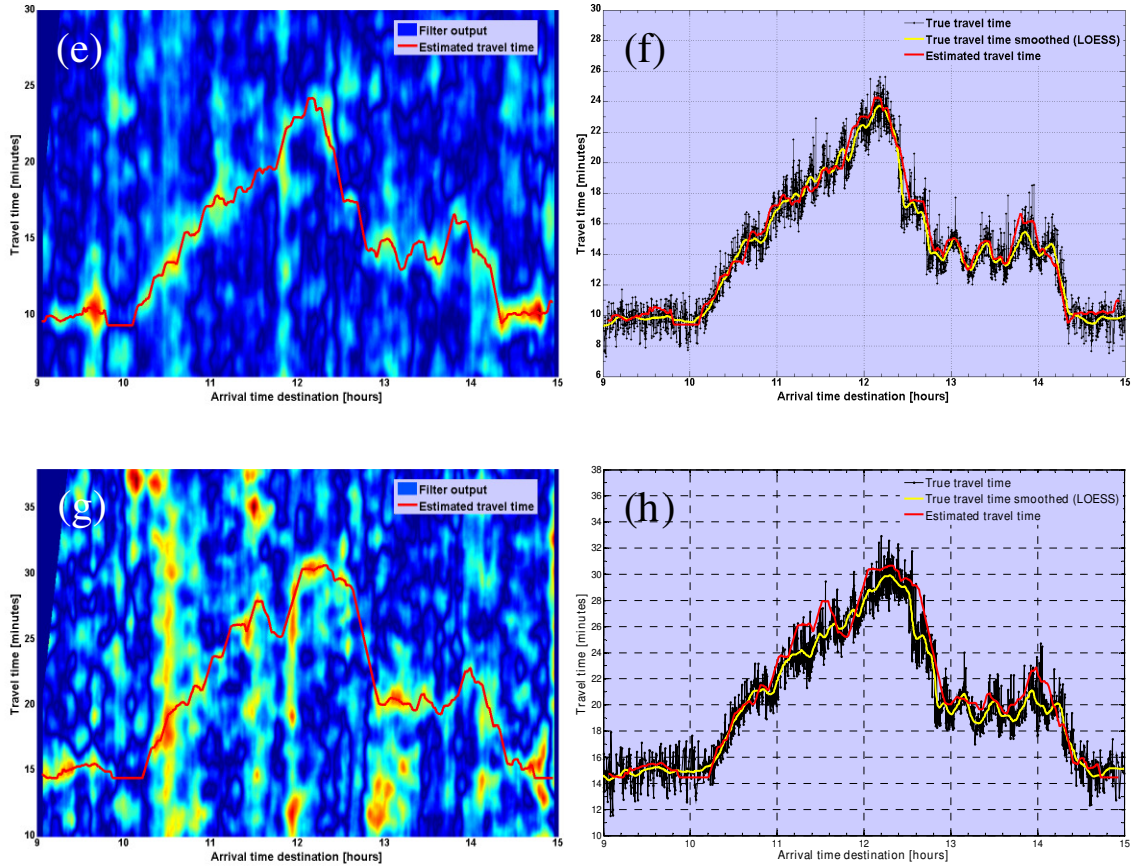

The plots on the left side in Figure 9 (a, c, e, and g) show the filter outputs together with the estimated travel times (red line), and the actual travel times for the four investigated origin-destination combinations; The plots on the right side (b, d, f, h) show the actual travel times (black), the smoothed actual travel times (yellow line), and the estimated travel times (red line).

We see from the four plots on the right side, that for all origin-destination combinations *the estimated travel times are in very good accordance with the actual travel times*. We can observe, that with increasing origin-destination distance (plots from top to bottom) the filter output contains an increasing number of unfeasible areas with high scores. This results from the fact, that the number of matches increases with distance. However, the algorithm can handle even these situations reliably.

4.2 Method 2: Travel time estimation with global sequence alignment

We have used the global alignment procedure on real life data and got plausible results. However, since we did not know the real travel times for these data we have assessed the algorithm with simulated data, which were done on the same segment from which we

analyzed real data (see Figure 7 and 8). For the simulated data we know for each vehicle which passes both detectors the actual travel time. However we have only used the time stamps and the noisy length information for the global alignment procedure. As scoring system we used the following setting: match reward = 20, mismatch penalty= –6, insertion and deletion penalty = –4, gap penalty for overlapping ends = –2. In the following graphs we see the actual travel time together with the estimated travel time plotted against the time at destination for 4 different destination detectors which are 4.8 km, 9.3 km, 12.8 km, and 19.6 km from the first detector apart. It is striking that the estimated travel time describes quite accurate the actual travel time distributions despite the extreme traffic situation and several unobserved ramps. Not until a distance of almost 20km the procedures starts to get difficulties at some time ranges.

Figure 10 Estimation results for four OD-combinations a) O1→D2 actual and estimated travel time; b) O1→D4 actual and estimated travel time; c) O1→D6 actual and estimated travel time; d) O1→D8 actual and estimated travel time.

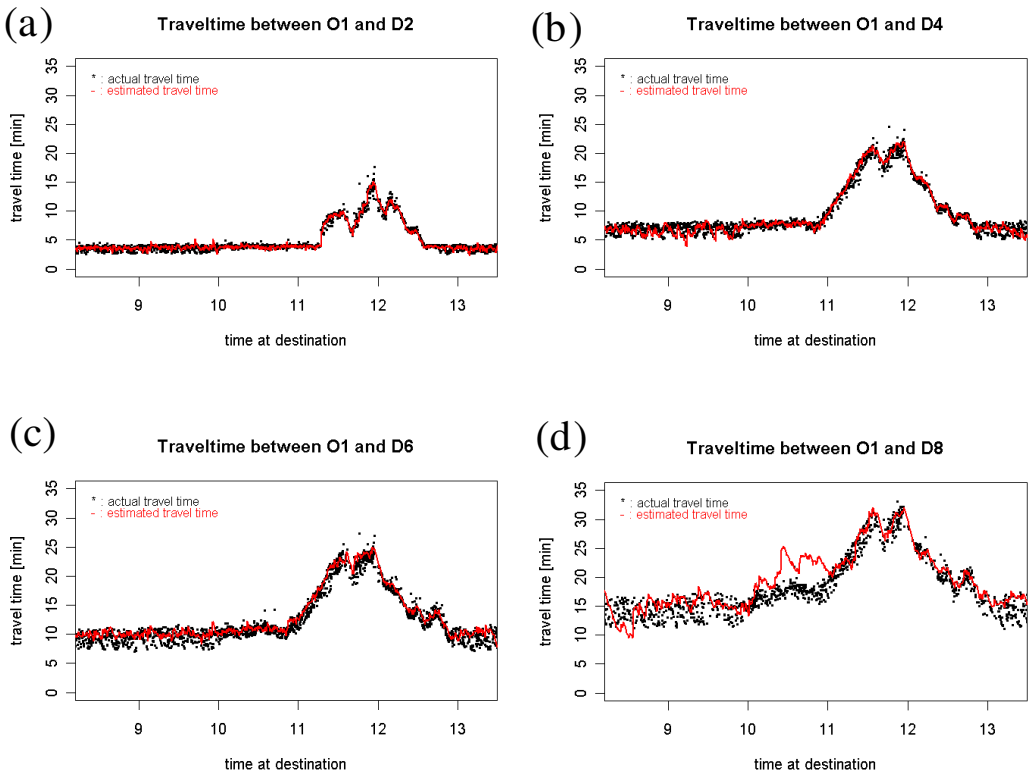

5. Summary and outlook

In this paper we presented two novel travel time estimation methods, which both use only vehicle lengths (e.g., from double inductance loops) and the appropriate time stamps at the detector stations as input. We performed tests with simulated single vehicle data, for origin-destination distances between 5 and 20 kilometres. Furthermore, depending on the OD-combination, up to four unobserved on- and off-ramps were part of network under investigation.

With both methods we could show, that for the investigated origin-destinations combinations *all relevant characteristics of the travel time trends were captured* and that the accuracies are thus within a well acceptable ranges.

Besides the fact that both methods work well even under hindered conditions (long distances, unobserved on- and off-ramps), some additional practical benefits of the methods are: (i) Provided that single car data are available at the detectors stations with sufficient accuracy, no additional infrastructure investments; (ii) Both methods work fully anonymous, i.e. no privacy issues arise; (iii) extensions to use more sophisticated detection technologies that provide additional vehicle features, are straightforward; (iv) with the presented quality of the travel time estimations, this forms a good basis for any travel time prediction method.

Future research on this topic will include the following major points:

- Application of the methods on real data sets together with an optimisation of the model parameters,
- A quantitative assessment of the accuracy of the travel times estimates for both methods,
- Performing tests for small distances with larger measurement errors assumed,
- Combing the two approaches,
- Improving the methods regarding robustness, and finally
- integrate the methods to field applications.

6. References

Abdulhai, B., S. M. Tabib (2003) Spatio-temporal inductance-pattern recognition for vehicle re-identification. Transportation Research Part C, 11 (3-4), 223-239.

Coifman, B. (1998a) A new algorithm for vehicle reidentification and travel time measurement on freeways, in: Proceedings of the 5th International Applications of Advanced Technologies in Transportation Engineering ASCE, 167-174.

Coifman, B. (1998b) Vehicle reidentification and travel time measurement in real-time on freeways using the existing loop detector infrastructure. Transportation Research Record, 1643, 181-191.

Coifman, B. (2002) Estimating travel times and vehicle trajectories on freeways using dual loop detectors. Transportation Research Part A, 36 (4), 351-364.

Coifman, B., M. Cassidy (2002) Vehicle reidentification and travel time measurement on congested freeways. Transportation Research Part A, 36 (10), 899-917.

Coifman, B., E. Ergueta (2003) Improved vehicle reidentification and travel time measurement on congested freeways. ASCE Journal of Transportation Engineering, 129 (5), 475-483.

Coifman, B., S. Krishnamurthy (2007) Vehicle reidentification and travel time measurement across freeway junctions using the existing detector infrastructure. Transportation Research Part C, 15 (3), 135-153.

Kwon, T. M. (2006) Blind deconvolution processing of loop inductance signals for vehicle reidentification. In: Proc. of the 85th Annual Meeting of the Transportation Research Board.

Needleman, S. B., Ch. D. Wunsch (1970) A general method applicable to the search for similarities in the amino acid sequence of two proteins. J. Mol. Biol., 48, 443-453.

Pfannerstill, E. (1984) A pattern recognition system for the re-identification of motor vehicles, in: Proceedings of the 7th IEEE International Conference on Pattern Recognition, Montreal, New Jersey, 553–555.

Rubin, M. (2007) Personal communication. Federal Roads Office (FEDRO).

Taxomex (1999) Datenblatt Schlaufenkarte zu Marksman M660. Taxomex S.A., Nyon, Schweiz.

Acknowledgements

The authors would like to thank the executive board of the IDP for financial support of this project. We would also like to thank the CTI (Swiss Innovation Promotion Agency) and Siemens Switzerland Ltd. for financial support of a preceding project on this topic (Grant number KTI 6949.2 FHS-ES). Finally we want to thank our colleagues at IDP, at Munich University of Technology, Chair of Traffic Engineering and Control (Axel Leonhardt, Matthias Spangler and Friedrich Maier), and at IMS (Institute of Mechatronic Systems at ZHW; Dejan Seatovic and Rolf Grüninger), for fruitful and inspiring discussions, which helped to improve the quality of this work.